Journal of Power Sources 237 (2013) 58–63

Contents lists available at SciVerse ScienceDirect

Journal of Power Sources

journal homepage: www.elsevier.com/locate/jpowsour

Electricity production and electrochemical impedance modeling of microbial fuel cells under static magnetic field

Yao Yin, Guangtuan Huang*, Yiran Tong, Yongdi Liu, Lehua Zhang

School of Resources and Environmental Engineering, East China University of Science and Technology, Shanghai 200237, China

HIGHLIGHTS

- MFCs were exposed to magnetic fields to improve the electricity production.
- The influences of magnetic fields with different intensities were investigated.
- Each component of reactors was tested by EIS.
- The equivalent circuit to fit EIS of whole cell is on the basis of those of anode and cathode.
- The primary influence of magnetic field on MFCs is the reduction of anode activation loss.

ARTICLE INFO

Article history:
Received 16 November 2012
Received in revised form
25 February 2013
Accepted 28 February 2013
Available online 14 March 2013

Keywords:
Microbial fuel cell
Magnetic field
Power density
Electrochemical impendence spectroscopy
Charge transfer resistance

ABSTRACT

Two-chamber microbial fuel cells (MFCs) were exposed to static magnetic field (MF) of field strengths 0 mT, 100 mT, 200 mT, and 300 mT, and the electricity production of the MFCs under the influence of the MF was investigated using electrochemical methods. The results show that the start-up periods of MFCs in MF were shorter than that without. The MFC with a 100-mT MF needed the shortest time (7 days) to obtain a stable voltage output. The maximum power density of 1.56 W m^{-2} was for a field strength of 200 mT, which was the best among the MFCs. The impact of the MF on the charge transfer resistances (R_{ct}) of the anode, cathode, and whole MFC was analyzed by electrochemical impedance spectroscopy (EIS). A new method was developed to extend the equivalent circuit (EC) model to the whole MFC by connecting the anode and cathode models in series. The simulated results show that anode R_{ct} values are much higher compared than at the cathode. The cell and anode R_{ct} values were reduced by 56.6% and 57.2%, respectively, for the 200-mT MF. It was also found that there is an optimal intensity MF range for the microorganisms.
© 2013 Elsevier B.V. All rights reserved.

1. Introduction

Microbial fuel cell (MFC) technology can exploit biodegradable material in organic wastewater for energy recovery [1,2]. MFCs overcome some of the inherent shortcomings of traditional biological wastewater treatment and may be able to mitigate water pollution as well as energy shortage problems to a certain extent. MFCs, which can be considered as a type of biofuel, have attracted the attention of universities, corporations, and governmental departments. However, at present, the power output of MFCs is too low, and cannot meet the power supply requirements of wastewater treatment facilities. Much research is being conducted to improve the power output and electricity production efficiency of MFCs through a variety of methods, such as looking for efficient exoelectrogens [2], modifying the electrode materials [3], improving the cell configuration [4], and applying a physical field [5].

Recently, the effect of a magnetic field (MF) on the electricity production of MFCs has been gaining attention. It has been proved that a MF can induce a series of biological reactions in microorganisms [6,7]. MFs can affect the characteristics of an enzyme, DNA, or biofilm, and thus affect the metabolism of the organism [8,9]. The application of these effects in biological wastewater treatment has been widely reported. Li et al. [5] found that a 100-mT MF promoted electricity production of Shewanella-inoculated MFCs, and the maximum voltage increased by 20–27%. The improvements in electricity production of MFCs exposed to MFs were mainly attributed to the enhanced bioelectrochemical activity, possibly through the oxidative stress mechanism.

Electrochemical impedance spectroscopy (EIS) is an electrochemical measurement method in which a small amplitude sine wave potential (or current) is used as a disturbance signal [10], and it

* Corresponding author. Tel.: +86 21 64252901.
E-mail address: gthuang@ecust.edu.cn (G. Huang).

0378-7753/$ – see front matter © 2013 Elsevier B.V. All rights reserved.
http://dx.doi.org/10.1016/j.jpowsour.2013.02.080

is a powerful tool in the research of MFCs [11–13]. It can be used to measure the cell internal resistance, but more importantly, it can also distinguish three contributions to the internal resistance: ohmic resistance, charge transfer resistance, and diffusion resistance [14]. In addition, EIS can be used to study the electrochemical behavior of the redox mediator secreted by bacteria in MFCs [15]. The most desirable feature of the application of EIS in MFC research is that no interruption or interference to the reactors and microbial cultivation is caused by the testing process.

However, there are currently two problems with the application of EIS in MFC research. First, the frequency range is not well defined, and it differs among studies [16,17]. Generally, the impedance value at high frequency represents ohmic resistance, and the impedance value at the lowest frequency is the total resistance [18]. Therefore, different measurement frequencies will influence the determination of the internal resistance. Second, although there is a basic form of the EIS equivalent circuit (EC), it is not sufficient for describing different MFC systems [14]. The differences in the structure and materials will be reflected in the EIS results. Sometimes, the fitting of the impendence results is not good due to the application of the basic fitting model [11]. In addition, the use of the basic model does not provide a complete analysis of the anode and cathode impedance.

EIS was used to study the electrochemical behavior of the MFC anode, cathode and whole MFC in this work. This was not only to establish a suitable equivalent circuit for the MFC, but also to analyze the impact of a magnetic field on each component of the MFC by fitting anode and cathode impedance results. In this study, the electricity production of sewage-inoculated two-chamber microbial fuel cells under different MF intensities was investigated. The results could provide valuable information for industrial applications of magnetic-field promoted MFC electricity production in wastewater treatment.

2. Experimental

2.1. MFC configuration and operation

Two-chamber MFCs were constructed using carbon cloth (Xinka Carbon Technology Co., Ltd., Shanghai, China) for the anode and cathode. The anode and cathode chambers were plexiglass cylinders (φ 4 × 6 cm, empty bed volume of approximately 75 mL each) adjoined at the flange, which contained the proton exchange membrane (NafionTM117, Dupont Co., Delaware, USA). The electrodes (2.5 × 2.5 cm, 6.25 cm^2), separated by a distance of approximately 9 cm, were connected by titanium wire. Four reactors were set up for the experiments, MFC0, MFC1, MFC2, and MFC3, which represent the MFCs under MFs of 0 mT, 100 mT, 200 mT, and 300 mT, respectively. The magnets were attached to the external walls of the anode chambers to obtain specific MF intensities at the anode position. A schematic diagram of the MFC experimental set up is shown in Fig. 1.

The MFCs were inoculated with a mixture (50/50 v/v) of equalization tank effluent from the sewage treatment plant of the East China University of Science and Technology (Shanghai, China) and a phosphate buffer solution (PBS, 50 mM) containing 1 g L^{-1} of sodium acetate and a mineral solution (12.5/1000 v/v) [19]. The catholyte consisted of 0.1-mM $K_3Fe(CN)_6$ in a 50-mM phosphate buffer solution. The anolyte and catholyte were kept in a 1-L brown reagent bottle and continuously recirculated into the MFC compartments using a peristaltic pump (BT100-1L, Longer Precision Pump Co., Baoding, China) at a flow rate of 2 mL min^{-1}. One gram of sodium acetate was added to the anolyte bottle every 2 days of the cycle, and the anodic and cathodic solutions were replaced every week. Electricity generation experiments were conducted at ambient temperature (25 °C).

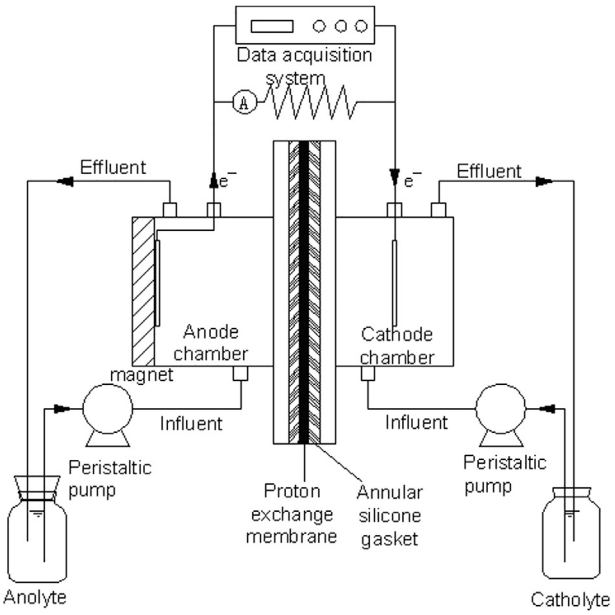

Fig. 1. Schematic diagram of MFC experimental installation loaded with MF.

2.2. MFC analysis

The MFCs started up with a fixed external resistance of 1000 Ω, and the voltage outputs were recorded by a computer every 5 min using a data acquisition system (Keithley 2701, Keithley Company, USA). During the startup period, the open circuit voltage was measured with a disconnected circuit three times each week. The polarization and power density curves were determined by linear scanning to investigate the influence of the exposure of MFCs to MFs on the energy efficiency. The linear scanning method adopted a two-electrode system, in which the cathode was used as the working electrode and the anode as the reference electrode and counter electrode. The circuits were disconnected until the MFC voltage stabilized to the open circuit voltage (OCV), and then the MFCs were scanned from the OCV to 10 mV at a scanning rate of 1 mV s^{-1}. The voltage (U) and current (I) were recorded to obtain the polarization curves. The power density curves were plotted using the relationship, $P = U \times I$.

Electrochemical impedance spectroscopy (EIS) was carried out using an electrochemical workstation (PARSTAT 2273, PAR, USA). The two-electrode mode was used to analyze the whole cell. The anode was used as the working electrode, and the cathode as the counter and reference electrodes. The three-electrode mode was used to analyze the individual electrodes. The electrode being examined was used as the working electrode, while the other electrode was the counter electrode. The saturated calomel electrode (SCE) was used as the reference electrode and was placed in the working electrode's compartment [14]. Impedance measurements were conducted at the OCV of MFCs over a frequency range of 100 kHz to 1 mHz. The Nyquist plots of the impedance spectra were analyzed using Zsimpwin 3.10 (Echem Software).

3. Results and discussion

3.1. Effect of MFs on MFC startup

Fig. 2 shows the voltage change from start to stable operation. The trends of the curves are consistent with the general observations of the startup of MFCs. The peaks of the curves indicate the

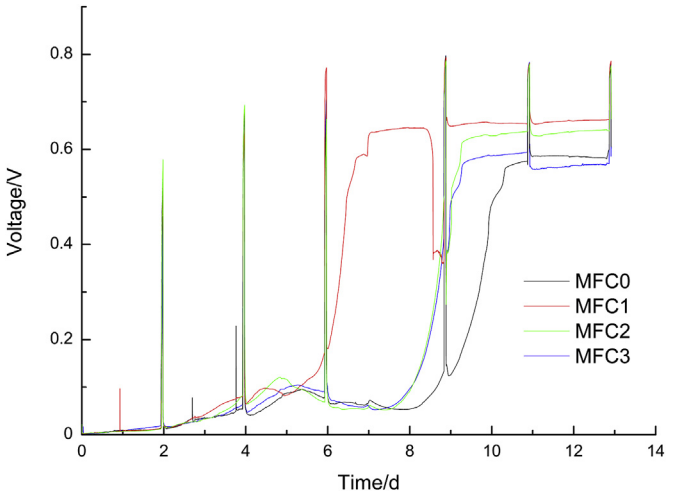

Fig. 2. MFCs voltage outputs change during the startup period with 1000 Ω external resistance (the peaks of curves indicate open circuit voltage when the circuit is disconnected).

OCV measured with a disconnected circuit. MFC1 started fastest with the 100-mT MF, for which the voltage changed suddenly on day 6 and finished startup on day 7. For MFC2 and MFC3 with MFs of 200 mT and 300 mT, respectively, the voltage jump occurred on day 7 and startup was completed on day 10. The voltage of MFC0 with no MF began to increase sharply on day 9 and achieved stability on day 11. These results show that the MF promoted the enrichment of anode electrogenesis and accelerated the rate of proliferation. It is thought that the role of the magnetic field is to reduce anode activation loss, which results from microbial metabolic activity and electrochemical reactions. In addition, considerably improved voltage outputs were found for the MFCs with 100-mT and 200-mT MFs and external resistances of 1000 Ω, as shown in Fig. 2. This also demonstrates the enhancement of electricity production in the presence of the MF.

3.2. Polarization and power density curves

The polarization curves are shown in Fig. 3a. As the current density increases, the cell voltage decreases. MFC polarization includes the anode, cathode, membrane, and electrolyte polarizations [18]. Owing to the same electrolyte and MFC construction, the MFC polarization curve could also be used to elucidate the performance of anode electrical production. From the polarization curves, it can be seen that the open circuit voltage of the reactors in the presence of a MF is higher than the value of MFC0 with no MF (Table 1). The ideal polarization curve can be divided into three regions: activation polarization at high current density, concentration polarization at low current density, and ohmic polarization in the intermediate linear region [20]. However, the concentration polarization is not evident here, which indicates that ohmic polarization governs the low current-density range.

The maximum power density is usually used to measure the capacity of electricity production. In Fig. 3b, the production performances of MFC1 and MFC2 were better than the other two reactors. The maximum power density of MFC2 was 1.56 W m^{-2} at a current density of 0.44 mA cm^{-2}, which was the best performance among the MFCs. According to Ohm's law, the power density of the cell reaches its maximum when the internal resistance is equal to external resistance. Thus, the internal resistances were calculated as shown in Table 1. The internal resistance of 129 Ω for MFC2 was the lowest.

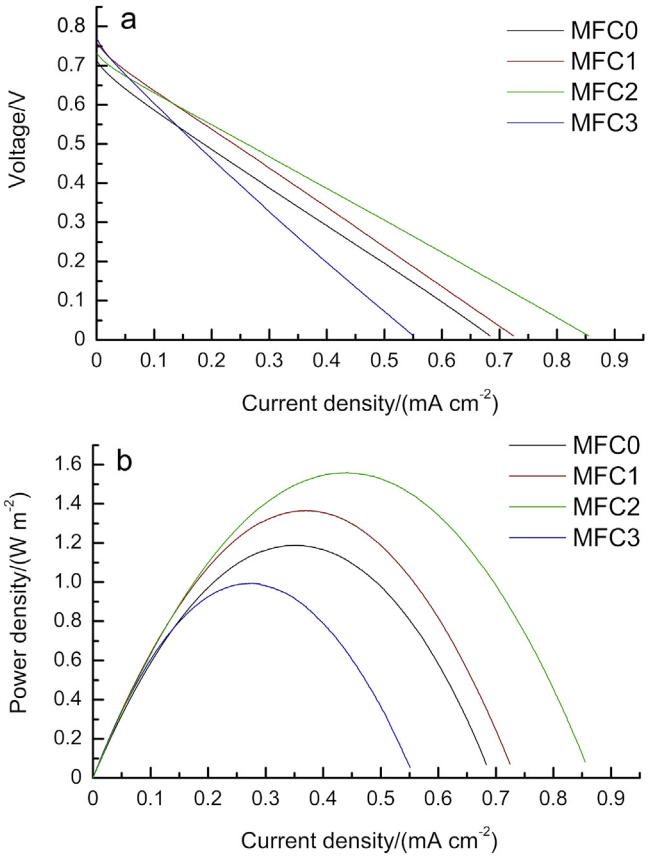

Fig. 3. Polarization (a) and power density (b) curves of MFCs.

3.3. Analysis of the charge transfer resistance (R_{ct}) by EIS

After the reactor startup, the electrochemical impedance spectroscopy of the anodes, cathodes, and whole cells was tested. Appropriate equivalent circuits were used to analyze the internal resistance.

The internal resistance of the MFC can be divided into three parts, as shown in Fig. 4. The resistors are in parallel with constant phase elements (CPE), which represent the anode and cathode. The resistance between the anode and cathode represents the electrolyte resistance. Owing to the dispersion effect, the electric double layer deviates from the ideal electric double layer, and hence, constant phase elements were used to replace the capacitors. The impedance spectra of the whole MFC were analyzed by fitting to the EC: (RC)R(RC). For MFC0, the simulation result is shown in Fig. 4.

In Fig. 4, there are three circular arcs over the high-, medium-, and low-frequency ranges in the Nyquist plot for MFC0 (the shape of the EIS curve is similar). From the simulation results, it can be seen that the calculated plots show similar trends to the measured

Table 1
Comparison of performance of four MFCs.

MFC	Open circuit voltage (V)	Maximum power density (W m^{-2})	Internal resistance (Ω)
MFC0	0.711	1.19	153
MFC1	0.759	1.37	161
MFC2	0.732	1.56	129
MFC3	0.769	0.99	210

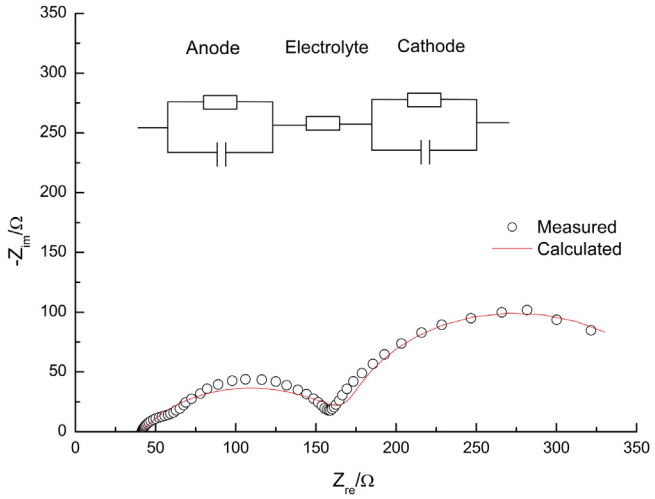

Fig. 4. The fitting result of MFC0 based on equivalent circuit (RC)R(RC).

plots. However, the arcs over the high- and low-frequency ranges are not well fitted. The chi-squared test parameter (Chi^2) is 2.05×10^{-3}. The model of the whole-cell impedance spectrum was symmetric between the anode and cathode [18]. Therefore, we established EIS equivalent circuits for the anode and cathode, and then, we connected the anode and cathode models in series to obtain the equivalent circuit for the whole cell.

Electrode potential losses originate from three sources: activation losses, ohmic losses, and mass transfer losses [21]. The equivalent circuit of the anode is shown in Fig. 5a. R_1 represents the ohmic resistance, and R_2 represents the charge transfer resistance. R_3 and C_3 in parallel represent the finite diffusion [11]. In Fig. 5a, it can be seen that the EIS result was well fitted. The diameter of the semicircle over the high-frequency range corresponds to the charge-transfer resistance.

It was found that there is only one semicircle over the high-frequency range in the cathode EIS results, which indicates that there was no obvious diffusion effect. The diameter of the semicircle still represents the resistance. Thus, the cathode internal resistance is divided into the ohmic resistance, R_1, and charge transfer resistance, R_2, in series. The results of the fitting are shown in Fig. 5b.

Based on the well-fitted simulation results for the anode and cathode, we constructed the equivalent circuit for the whole cell. EC3 is shown in Fig. 5c. R_1 denotes the ohmic resistance, R_{2a} and R_{3c} express the charge transfer resistance of the anode and cathode, and R_4 and C_4 are related to the finite diffusion, similarly to the R_3C_3 term in EC1. It can be seen from Fig. 5c that the fit has been greatly improved. The chi-squared test parameter dropped to 9.18×10^{-5}. This infers that our equivalent circuit, constructed by connecting the anode and cathode models, is suitable for the analysis of impedance spectra, which has not been reported previously. Through the above method, better simulation results were obtained for the other reactors and these are shown in Fig. 6.

It is known that electrogenesis plays the role of a catalyst, which primarily causes the activation loss of the catalyzed reaction in the MFC [22,23]. We chose the charge transfer resistance to investigate the influence of the MF intensity. The charge transfer resistance data for the anode, cathode, and cell can be obtained by fitting, as shown in Fig. 7. The resistance of the whole cell is given by R_{2a} plus R_{3c}. It can be seen that the anode R_{ct} was much higher than that of the cathode, which indicates that anode limitations dominate cell activation losses. The reason is that using $K_3[Fe(CN)_6]$ as the catholyte results in a high mass-transfer efficiency and low activation potential.

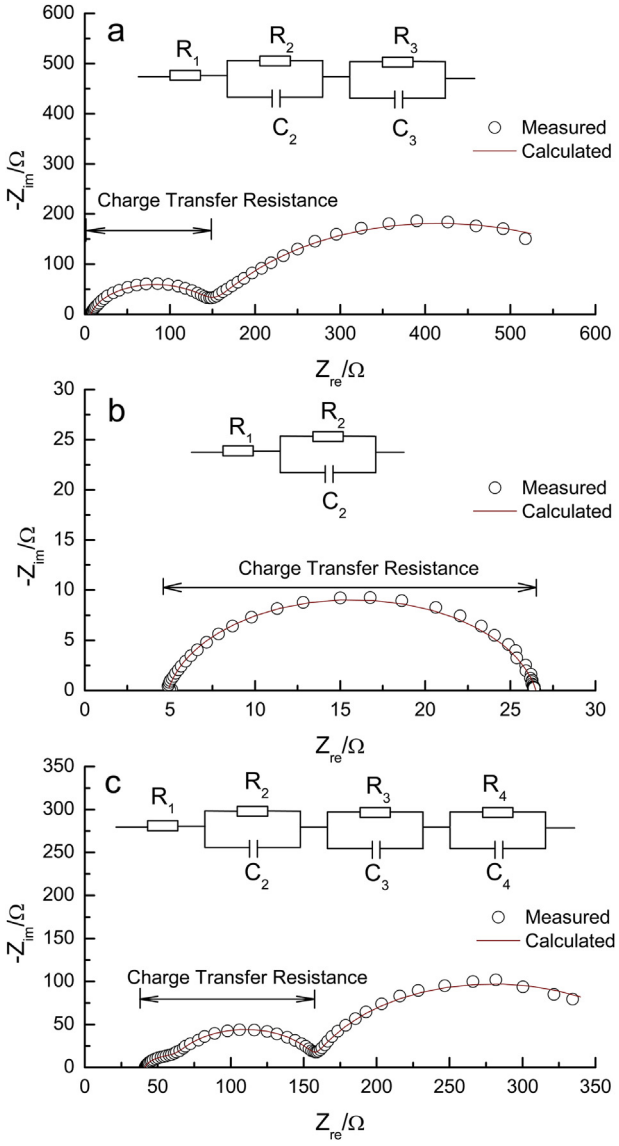

Fig. 5. The fitting results of MFC0 Nyquist plots. (a) Anode EC1: $R_1(R_2C_2)(R_3C_3)$; (b) cathode EC2: $R_1(R_2C_2)$; (c) whole cell EC3: $R_1(R_{2a}C_{2a})(R_{3c}C_{3c})(R_4C_4)$.

Further comparison shows that the cell R_{ct} values of MFC1 and MFC2 were less than those of MFC0 and MFC3, with the minimum value being 50.10 Ω for MFC2. The cathode R_{ct} values for the various reactors were relatively close at 21.60, 28.41, 24.77, and 14.52 Ω for MFC0, MFC1, MFC2, and MFC3, respectively. The anode R_{ct} showed clear differences among the four MFCs, $R_{ct2} < R_{ct1} < R_{ct3} < R_{ct0}$ which were consistent with the R_{ct} values of the cell. Compared to MFC0, the cell R_{ct} and the anode R_{ct} of MFC2 were reduced by 56.6% and 57.2%, respectively. When the MF intensity reached 300 mT, the effect of the magnetic field in reducing the charge transfer resistance was not obvious.

From these results, it can be seen that a static magnetic field can decrease the anode charge transfer resistance, and thus reduce the overall charge transfer resistance of the cell. The primary influence of the magnetic field on MFCs is the reduction of anode activation loss. Li et al. [5] conjectured that the effect of the magnetic field is to reduce the energy loss of electron transfer, which maybe the result in changing the rate of bioelectrochemical reaction. However, the reduction of R_{ct} is not only related to extracellular microbial electron-transfer activity, but may also be influenced by other

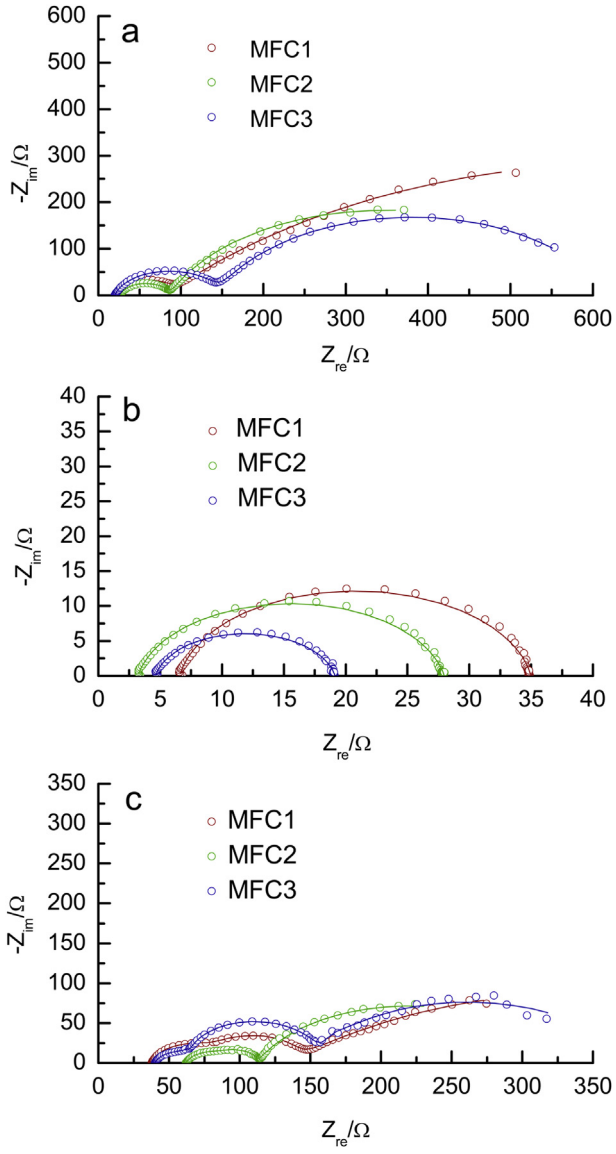

Fig. 6. The fitting results of MFC1–3 Nyquist plots. (a) Anode EC1: $R_1(R_2C_2)(R_3C_3)$; (b) cathode EC2: $R_1(R_2C_2)$; (c) whole cell EC3: $R_1(R_{2a}C_{2a})(R_{3c}C_{3c})(R_4C_4)$.

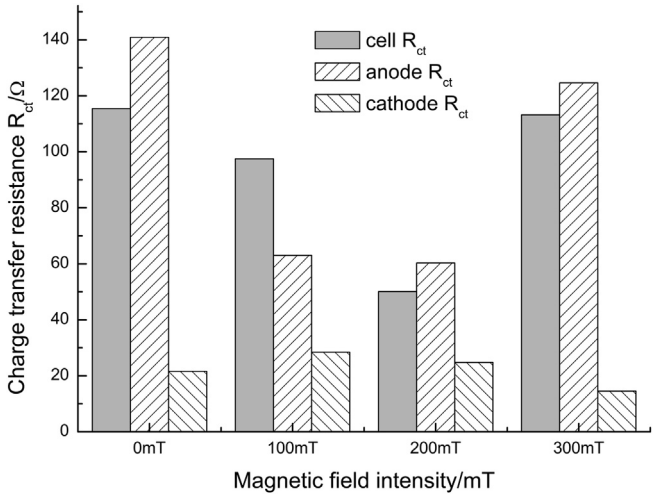

Fig. 7. Simulated values of charge transfer resistance R_{ct}.

factors, such as the anode biomass [24]. This requires further investigation using other techniques, such as cyclic voltammetry and biomass measurements.

There are two main processes at the anode of MFCs: electron generation via microorganisms degrading (oxidizing) the substrate and electron transfer from microorganisms to the electrode. Under the specific conditions of the electrode materials, reactor configuration, and electrolyte, the two processes lead to anodic activation losses, and influence the MFC voltage. Based on the analysis of the electrochemical impedance results in our research, the static magnetic field decreased the anode charge transfer resistance, and thereby reduced the whole cell charge transfer resistance. The charge transfer resistance is affected by the kinetics of the electrode reactions [14]. Therefore, the possible mechanism could involve changes in the rates of bioelectrochemical processes upon exposure of the MFCs to the MF. It has been reported that the effects of a MF on the activity of activated sludge in wastewater treatment is the enhancement of the substrate removal rate [25,26]. This suggests that the MF affects the microbial metabolic process. Additionally, cytochrome C, which is a hemoglobin-containing metal protein located on the cell membrane and is an important part of the respiratory chain, is one of the main pathways for the electron transfer process [27]. It is known that MFs can affect the characteristics of proteins in microorganisms [6], and thus, it should be considered MF might affect cytochrome C and thereby affect the electron transfer process.

Additionally, we found that the effects of 100-mT and 300-mT MFs were lower than those of the 200-mT MF. Many studies have found that MFs can promote or inhibit microorganisms at different intensities [28,29]. Perhaps, the effect of a low magnetic field with low energy on the microorganism is not obvious, and a strong magnetic field harms the bacteria leading to inactivation [28]. Therefore, it can be concluded that there is an optimal magnetic-field intensity range for the microorganisms, which can be determined by analyzing the impendence characteristics. If the magnetic-field intensity is too low or too high, no improvement will be seen.

In this research, the impact of magnetic fields on the microorganisms in MFCs has been confirmed. However, according to previous studies, MFs also have effects on the electrical behavior of $[Fe(CN)_6]^{3-}$ and on the oxygen reduction reaction [30–32]. The influence of the magnetic field on the MFC cathode also needs to be explored further to comprehensively understand the application of magnetic fields in MFCs.

4. Conclusions

This study has shown the impact of MFs on the electricity production and impedance behavior of two-chamber MFC inoculated with mixed bacteria. The production performances of the MFCs exposed to MFs of 100 mT and 200 mT were better than those of the other two reactors. The best performance was for the MFC with a 200-mT MF, which had a power density of 1.56 W m^{-2} at a current density of 0.44 mA cm^{-2}. The method of using the equivalent circuit to fit the EIS of the whole cell on the basis of the anode and cathode models improves the accuracy of the EIS fit significantly. The impact of 100-mT and 200-mT MFs was to reduce the R_{ct} values of the anode and of the whole cell, and was determined by comparing the charge-transfer resistance of the anode, cathode, and whole cell. This implies anode activation losses in the MFC decrease as a result of exposure to the MF. Nevertheless, the improvement for the 300-mT MF was not significant. Thus, the exact mechanism of the effects of MFs on MFCs needs further investigation.

Acknowledgments

The authors wish to thank National Natural Science Foundation of China (51078144) for the financial support of this study.

References

[1] E.F. Ashley, P.N. Kelly, Energies 3 (2010) 899–919.
[2] B.E. Logan, Nat. Rev. Microbiol. 7 (2009) 375–381.
[3] M. Zhou, M. Chi, J. Luo, H. He, T. Jin, J. Power Sources 196 (2011) 4427–4435.
[4] S. Cheng, H. Liu, B.E. Logan, Environ. Sci. Technol. 40 (2006) 2426–2432.
[5] W. Li, G. Sheng, X. Liu, P. Cai, M. Sun, X. Xiao, Y. Wang, Z. Tong, F. Dong, H. Yu, Biosens. Bioelectron. 26 (2011) 3987–3992.
[6] R.L. Moore, Can. J. Microbiol. 25 (1979) 1145–1151.
[7] O.R. Justo, V.H. Perez, D.C. Alvarez, R.M. Alegre, Appl. Biochem. Biotechnol. 134 (2006) 155–163.
[8] H. Sahebjamei, P. Abdolmaleki, F. Ghanati, Bioelectromagnetics 28 (2007) 42–47.
[9] A.E. May, S. Snoussi, N.B. Miloud, I. Maatouk, H. Abdelmelek, R.B. Aissa, A. Landoulsi, Foodborne Pathog. Dis. 5 (2009) 547–552.
[10] F. Zhao, R.C.T. Slade, J.R. Varcoe, Chem. Soc. Rev. 38 (2009) 1926–1939.
[11] Z. He, N. Wagner, S.D. Minteer, L.T. Angenent, Environ. Sci. Technol. 40 (2006) 5212–5217.
[12] Y. Qiao, C.M. Li, S.J. Bao, Q.L. Bao, J. Power Sources 170 (2007) 79–84.
[13] S. You, Q. Zhao, J. Zhang, J. Jiang, C. Wan, M. Du, S. Zhao, J. Power Sources 173 (2007) 172–177.
[14] Z. He, F. Mansfeld, Energy Environ. Sci. 2 (2009) 215–219.
[15] R.P. Ramasamy, V. Gadhamshetty, L.J. Nadeau, G.R. Johnson, Biotechnol. Bioeng. 104 (2009) 882–891.
[16] S. Jung, M.M. Mench, J.M. Regan, Environ. Sci. Technol. 45 (2011) 9069–9074.
[17] D. Aaron, C. Tsouris, C.Y. Hamilton, A.P. Borole, Energies 3 (2010) 592–606.
[18] A.P. Borole, D. Aaron, C.Y. Hamilton, C. Tsouris, Environ. Sci. Technol. 44 (2010) 2740–2745.
[19] S.A. Cheng, B.E. Logan, Electrochem. Commun. 9 (2007) 492–496.
[20] A.J. Bard, L.R. Faulkner, Electrochemical Methods: Fundamentals and Applications, second ed., John Wiley & Sons, New York, 2001.
[21] B.E. Logan, Microbial Fuel Cells, John Wiley & Sons, New Jersey, 2008.
[22] P. Clauwaert, P. Aelterman, T.H. Pham, L.D. Schamphelaire, M. Carballa, K. Rabaey, W. Verstraete, Appl. Microbiol. Biotechnol. 79 (2008) 901–913.
[23] B.E. Logan, B. Hamelers, R. Rozendal, U. Schroder, J. Keller, S. Freguia, P. Aelterman, W. Verstraete, K. Rabaey, Environ. Sci. Technol. 40 (2006) 5181–5192.
[24] R.P. Ramasamy, Z.Y. Ren, M.M. Mench, J.M. Regan, Biotechnol. Bioeng. 101 (2008) 101–108.
[25] H. Yavuz, S.S. Celebi, Enzyme Microb. Technol. 26 (2000) 22–27.
[26] A. Tomska, L. Wolny, Desalination 222 (2008) 368–373.
[27] D.R. Bond, D.R. Lovley, Appl. Environ. Microbiol. 69 (2003) 1548–1555.
[28] S. Liu, F. Yang, F. Meng, H. Chen, Z. Gong, J. Biotechnol. 138 (2008) 96–102.
[29] P.E. Kovacs, R.L. Valentine, P.J. Alvarez, Crit. Rev. Environ. Sci. Technol. 27 (1997) 319–382.
[30] G. Saravanan, K. Fujio, S. Ozeki, Magnetic Field Effects on Electric Behavior of $[Fe(CN)_6]^{3-}$ at Bare and Membrane-Coated Electrodes, Iop Publishing Ltd, Bristol, England, 2008.
[31] C. Choi, M. Kim, S.W. Hong, Y.S. Choi, Y.I. Song, S. Kim, H.J. Kim, Bull. Korean Chem. Soc. 31 (2010) 1729–1731.
[32] T. Okada, N.I. Wakayama, L. Wang, H. Shingu, J. Okano, T. Ozawa, Electrochim. Acta 48 (2003) 531–539.